

Accepted Manuscript

1, 3-Indanedione functionalized fluorene luminophores: Negative solvatochromism, nanostructure-morphology determined AIE and mechanoresponsive luminescence turn-on

Fang Zhang, Rong Zhang, Xiaozhong Liang, Kunpeng Guo, Zhaoxiang Han, Xiaoqing Lu, Jingjuan Xie, Jie Li, Da Li, Xia Tian

PII: S0143-7208(18)30226-2

DOI: [10.1016/j.dyepig.2018.03.059](https://doi.org/10.1016/j.dyepig.2018.03.059)

Reference: DYPI 6644

To appear in: *Dyes and Pigments*

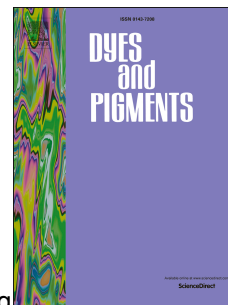
Received Date: 30 January 2018

Revised Date: 24 March 2018

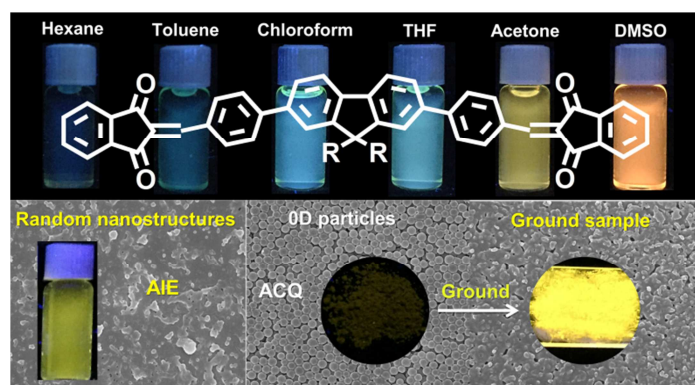
Accepted Date: 24 March 2018

Please cite this article as: Zhang F, Zhang R, Liang X, Guo K, Han Z, Lu X, Xie J, Li J, Li D, Tian X, 1, 3-Indanedione functionalized fluorene luminophores: Negative solvatochromism, nanostructure-morphology determined AIE and mechanoresponsive luminescence turn-on, *Dyes and Pigments* (2018), doi: 10.1016/j.dyepig.2018.03.059.

This is a PDF file of an unedited manuscript that has been accepted for publication. As a service to our customers we are providing this early version of the manuscript. The manuscript will undergo copyediting, typesetting, and review of the resulting proof before it is published in its final form. Please note that during the production process errors may be discovered which could affect the content, and all legal disclaimers that apply to the journal pertain.



Graphical Abstract



A series of 1, 3-indanedione functionalized fluorene luminophores simultaneously exhibit negative solvatochromism, AIE and mechanoresponsive luminescence turn-on were realized by taking the advantages of ICT and nanostructured morphological effects.

1, 3-Indanedione functionalized fluorene luminophores: Negative solvatochromism, nanostructure-morphology determined AIE and mechanoresponsive luminescence turn-on

Fang Zhang,^a Rong Zhang,^a Xiaozhong Liang,^a Kunpeng Guo,^{a*} Zhaoxiang Han,^b Xiaoqing Lu,^b Jingjuan Xie,^a Jie Li,^{a*} Da Li,^a Xia Tian^a

^a Ministry of Education Key Laboratory of Interface Science and Engineering in Advanced Materials, Research Center of Advanced Materials Science and Technology, Taiyuan University of Technology, Taiyuan 030024, P. R. China

^b College of Science, China University of Petroleum, Qingdao, Shandong 266555, China.

Corresponding Author: guokunpeng@tyut.edu.cn; lijie01@tyut.edu.cn

Abstract

Luminous efficiency in polar environment and aggregated state, as well as high-contrast luminescence on/off switching under external stimuli are significant issues to be addressed in developing functional fluorescent materials. Combining the advantages of solvatochromic effect in intramolecular charge transfer (ICT) compounds with their nanostructured morphological effects, we herein report a series of A- π -D- π -A fluorene derivatives, which simultaneously exhibit negative solvatochromism, aggregation-induced emission (AIE) and mechanoresponsive luminescence (MRL) turn-on. These molecules contain the same fluorene donor (D) and 1,3-indandione acceptor (A) but differ in alkyl substituents in the 9-position of the fluorene segment, including 9,9-dibutyl (***b*-DIPF**), 9,9-dioctyl (***o*-DIPF**) and 9,9-didodecyl (***d*-DIPF**). The emission colors of these compounds were changed from

blue to orange-red, and the fluorescence quantum yields increased upon increasing the solvent polarity from nonpolar hexane to polar dimethyl sulfoxide. Due to the formed random nanostructured aggregates, the compounds exhibited AIE characteristics in THF/H₂O mixtures. Oppositely, their emission quenched 0D particles which were afforded by quick evaporation of their dichloromethane solvents under vacuum displayed remarkable mechanoresponsive luminescence turn-on behavior. Our results suggest that rationally design ICT molecules and control their nanostructures would be promising way for realizing multifunctional fluorescent materials.

KEYWORDS: organic luminophores; nanostructure morphology; negative solvatochromism; aggregation-induced emission; mechanoresponsive luminescence turn-on

1. Introduction

Luminescent materials that not only give intense emission in both solvents and aggregate state, but also exhibit sensitive luminescent properties to external stimuli have attracted great interest due to their potential application in sensors, displays, memory storage and security technologies [1–4]. Among them, organic molecules with tunable donor (D) and acceptor (A) segments are promising candidates owing to their inherent intramolecular charge transfer (ICT) character and tunable molecular conformations based on which the modification of the intermolecular interactions in response to external stimuli could be realized [5–8]. Recently, some polarity-sensitive ICT fluorescent probes whose emitting colors can be tuned in a wide range of wavelengths are available [9–12]. However, most of the reported compounds exhibit

positive solvatochromism, whose emission intensity suffers from decrease with increasing the solvent polarity [10,11]. Consequently, the fluorescence tends to be quenched or weakened in polar environment. In addition, due to the adverse internal conversion, intersystem crossing, intermolecular electron transfer, as well as excimer or exciplex formation and isomerization, many ICT materials emit efficiently in dilute solution but weaken or quench in aggregated state [13–20]. These positive solvatochromism and aggregation-caused quenching (ACQ) greatly limit their real-world utilization, such as in polar biological systems. To solve these problems, developing negative solvatochromic luminescent molecules which simultaneously exhibit aggregation-induced emission (AIE) or aggregation-induced enhanced emission (AIEE) property is of great significance [2,21,22]. In this case, their emitting color redshifts while emission intensity increases upon increasing solvent polarity and forming aggregates.

Currently, organic mechanoresponsive luminescent (MRL) materials that change luminescent signals, such as emission colour and intensity, in response to external mechanical stimuli have drawn great attention due to their potential applications in mechano-sensors and security technologies [23–27]. In comparison with the materials that show mechanoresponsive dichromic switching or luminescence turn-off properties [28], those displaying emission turn-on response in reaction to external force stimulus are particularly intriguing because they permit the production of high-contrast signals [29-32]. Traditionally, most reported MRL materials are based on AIE active luminophores aiming to realize efficient solid-state emission [33-35],

which inhibits them to achieve high-contrast MRL turn-on behaviour. For our purpose, converting AIE materials to weak/non-emissive metastable solid would be a promising strategy towards MRL turn-on. However, it seems a challenging work because the contradictory fluorescent properties were combined into one system.

Recent studies demonstrated that the morphological engineering of the nanostructures could provide a rational control over the photophysical properties of luminescent materials [36-39]. Inspired by these, we aim to develop multifunctional materials with negative solvatochromism, AIE and MRL turn-on properties to achieve highly efficient luminescence in polar solvents and aggregated state, as well as high-contrast response to external mechano-stimuli based on their ICT effect and nanostructure morphologies. To achieve optimized performance, demonstrated here were three A- π -D- π -A fluorene derivatives with 1, 3-indandione acceptor but differing in alkyl substituents in the 9, 9-position of the donor fluorenyl group (***b*-DIPF**, ***o*-DIPF** and ***d*-DIPF**, Scheme 1). In comparison with the reported A- π -D- π -A carbazole derivatives with dicyanovinyl acceptor and one alky chain in the molecular backbone [40], herein suited electron-donating and withdrawing ability of fluorenyl and 1,3-indandione moieties endows the compounds with negative solvation effect, leading to increased fluorescence quantum yield (Φ_F) values from 0.7% in nonpolar hexane to 24.5% in polar DMSO accompanied with emission colour from blue to orange. Moreover, the moderately twisted skeleton and the two flexible alky chains yield diverse luminescent properties in the aggregate and solid states depending on their nanostructure morphologies. Different to the ACQ carbazole

derivatives, all fluorene derivatives formed random nanostructured aggregates in THF/H₂O mixtures that exhibit AIE active characteristics. On the contrary, by quick evaporation of dichloromethane solvent under vacuum the fluorene derivatives grew into metastable emission-quenched OD particles, which exhibited remarkable high-contrast luminescence turn-on upon mechanical grinding. By optimizing the alky lengths, *o*-DIPF realized the highest contrast ratio of MRL turn-on, whose Φ_F of the ground sample enhanced about 163-fold in comparison with that of the pristine OD particles. As a result, this work provides a new way for tuning ICT molecules with versatile fluorescent behaviors in different states.

2. Results and discussion

2.1. Materials and Methods

The target DIPF homologues were synthesized according to the literature using a three-step procedure (Scheme 1) [41-44]. Compounds **A1**, **A2** and **A3** were synthesized by the alkylation reaction of 2,7-dibromo-fluorene with 1-bromobutane, 1-bromooctane and 1-bromododecane, respectively. **B1**, **B2** and **B3** were obtained by Suzuki reaction of 4-formylphenylboronic acid with **A1**, **A2** and **A3**, respectively. Finally, *b*-DIPF, *o*-DIPF and *d*-DIPF were obtained by Knoevenagel condensation reaction of 1,3-indandione with **B1**, **B2** and **B3**, respectively. The chemical structures of *b*-DIPF, *o*-DIPF and *d*-DIPF were fully characterized by ¹H NMR, ¹³C NMR and mass spectrometry (Supporting Information for details). All of the compounds are soluble in common organic solvents such as CH₂Cl₂ and THF, but insoluble in water.

2.2. Theoretical calculations

To understand the molecular conformations and ICT characteristics of these compounds, the optimized molecular geometries and frontier orbital distributions were first evaluated by DFT calculation at the B3LYP/6-31G* level. All of the molecules adopted moderately twisted backbones with the dihedral angles between the phenyl bridge and the central fluorenyl unit of 36.4°/37.3°, 35.8°/36.7° and 36.3°/36.3° for ***b*-DIPF**, ***o*-DIPF** and ***d*-DIPF** (Fig. 1a, Fig. S1a and Fig. S2a), respectively. Meanwhile, the two flexible alky chains were found nearly perpendicular arranged to the molecular backbones. Taken together, such molecular configurations indicate that their fluorescent performances may be sensitive to the morphological effects [40,44]. For all the compounds, the highest occupied molecular orbitals (HOMOs) were mainly localized on the central fluorenyl core with sizeable distribution on the two phenyl rings, while the lowest unoccupied molecular orbitals (LUMOs) were more shifted to the 1,3-indandione acceptor units (Fig. 1b, Fig. S1b and Fig. S2b). Such spatial separation between the HOMO and LUMO supported a typical ICT effect between the electron donor and acceptor moieties.

2.3. Negative solvatochromic effect

The UV-Vis absorption and photoluminescence (PL) spectra were studied in solvents with different polarities and the corresponding data were extracted in Table 1. All compounds in various solvents exhibited similar absorption maxima (Fig. 2a, Fig. S3a and Fig. S4a). The absorption bands in the range of 410-450 nm were mainly attributed to the intramolecular charge transfer (ICT) transition. The absorption maxima (λ_{Abs}) of ***b*-DIPF**, ***o*-DIPF** and ***d*-DIPF** were red-shifted about 18-27 nm on

increasing the solvent polarity from hexane to DMSO, which indicated a small change in dipole moment in the ground state. Meanwhile, it was observed the variations of their absorption Full Width at Half Maximum (FWHM) were similar, which were increased from 74 nm to about 104 nm with increasing the solvent polarity, indicating more diversified electron transition pathways occurred in a more polar solvent. However, the variations of their absorptivity show solubility dependence. For ***b*-DIPF**, the molar extinction coefficient (ϵ) increases in moving from hexane to DMSO, owing to its relative poor solubility. While the ϵ of ***o*-DIPF** and ***d*-DIPF** are slightly decreased in same case due to the fact that the solubility and polarity of the compounds are increased and reduced, respectively, by the attachment of prolonged alkyl chains to the fluorene. Interestingly, the maximum emission peaks showed remarkable bathochromic shifts (> 130 nm) in the PL spectra accompanied with a distinct color change from blue to orange-red (Fig. 2b, Fig. S3b and S4b in the Supporting Information). According to the Lippert-Mataga equation (Equation S1 and Equation S2), plots of the Stokes shifts versus the orientation polarizability (Δf) of the solvent were illustrated (Fig. 2d, Fig. S3d and Fig. S4d), which showed one set of linearity indicative of one dominated ICT excited state maintained in various polarity of solvents [45-47]. Moreover, the slope values of the fitting line were calculated to be 10938 for ***b*-DIPF**, 11183 for ***o*-DIPF** and 11820 for ***d*-DIPF**, respectively, suggesting the dipole moment in the excited state was increased in a more polar solvent when the charges transferred from fluorenyl to 1,3-indandione unit. With the consequence that the polarized excited state is stabilized to adapt to the enhanced dipole moment

through the relocation of the polar solvent molecules, resulting in lowered energy and the red-shifted fluorescence.

In sharp contrast to the conventional ICT molecules that show a decreased Φ_F in polar solvent, **b-DIPF**, **o-DIPF** and **d-DIPF** display negative solvatochromic effect with an increased Φ_F as the solvent polarity is increased (Fig. 2c, Fig. S3c and Fig. S4c, Table 1). For instance, the Φ_F value of **o-DIPF** was increased from 0.7% in hexane to 24.5% in DMSO. Studies have suggested the negative solvatochromic effect may mainly arise from the “proximity effect” and “conformational change” [48,49]. For compounds studied in this work, their Stokes shifts were increased with the raise of the solvent polarity (Table 1). Correspondingly, a larger excitation-induced geometry change exists in polar solvents than nonpolar solvents, which would decrease the Φ_F . Therefore, the reduction of “proximity effect” of $\pi-\pi^*$ and $n-\pi^*$ transition of the molecules with the increased solvent polarity contributes the key factor to their strong emission in polar solvents. In comparison with our previous work [40], such reduction of “proximity effect” in herein fluorene derivatives can be reasonably attributed to the balanced electron-donating and withdrawing abilities of the donor and the acceptor moieties. As a result, the remarkable resolving ability (Fig. 2e, Fig. S3e and Fig. S4e), combined with the moderate fluorescent intensity, suggests the possible application of these compounds for solution-polarity detection. Take **o-DIPF** as an example, the Commission Internationale de l’Eclairage (CIE) color coordinates are located at (0.23, 0.25), (0.19, 0.27), (0.30, 0.46), (0.32, 0.51), (0.43, 0.49) and (0.51, 0.45) zones, with the increases the solvent polarity from hexane to

toluene, chloroform, THF, acetone and DMSO, respectively.

2.4. Random nanostructures determined aggregation induced emission

Structurally, the perpendicular arrangement of alkyl chains to the backbones may inhibit the intermolecular π - π interactions in aggregation, thus preventing or alleviating those nonradiative pathways and further giving intense emission in their aggregated states. To evaluate the possible AIE characteristics, their fluorescent behaviors in THF/H₂O mixtures were studied with different water fractions (f_w s) (Fig. 3, Fig. S5 and Fig. S6). As illustrated in Fig. 3a, 3b and 3c, the PL intensities and wavelengths of ***o*-DIPF** varied in different range of water fractions. When the f_w was increased from 0% to 60%, the maximum emission was followed by a red-shift of about 48 nm and a distinct color was changed from green to orange red. Such a red-shift can be attributed to ICT effect arising from the increased solvent polarity through an increase in the water fraction. The recorded UV-Vis spectra revealed the mixtures were homogeneous (Fig. 3d), suggesting the increased PL intensities stemmed from the “negative solvatochromic effect”. Further increasing the f_w led to a broadening and level off in the long wavelength region of the absorption spectra (Fig. 3d), indicating ***o*-DIPF** molecules aggregated into particles that scattered light. Correspondingly, blue-shifted of the maximum emission accompanied with color change from orange red to yellow were observed, which were assigned to the formed poor soluble aggregates due to the more hydrophobic environment [50]. Notably, the PL intensity was dramatically enhanced upon increasing the water fractions in the mixtures, indicating a typical AIE behavior (Fig. 3b and Fig. 3c). Scanning electron

microscopy (SEM) characterization further revealed the morphology of the aggregates. Random nanostructured aggregates were formed at an f_w of 90% (Fig. 3e), implying the adverse π - π interactions may be suppressed in the disordered motifs and as a result emission was enhanced.

2.5. 0D particles determined mechanoresponsive luminescence turn-on

After removing the dichloromethane solvent through rotary evaporation under vacuum, dark-yellow powders of ***b*-DIPF**, ***o*-DIPF** and ***d*-DIPF** were obtained. Different from their emissive aggregates that formed in THF/H₂O mixtures, the powders exhibited weak emissions at 563nm ($\Phi_F = 0.38\%$), 578nm ($\Phi_F = 0.12\%$) and 556nm ($\Phi_F = 0.25\%$) for ***b*-DIPF**, ***o*-DIPF** and ***d*-DIPF**, respectively (Fig. 4a, Fig. S7 and Fig. S9). Such distinctively luminescent performances allow us to make the speculation that their morphologies would be different from each other. SEM images support our hypothesis. 0D particles with diameters ranging from 300–500 nm were observed for the dark-yellow powders (Fig. 5a, Fig. S8a and Fig. S10a). Due to their moderate twisted molecular configuration, such ordered nanostructures have been proposed from the dominative *J*-aggregates of the molecules, in which unfavorable π - π stacking between the molecules caused emission quenching [51]. The differential scanning calorimetry (DSC) curves of the 0D particles displayed exothermic peaks at 117 °C ($\Delta H = 22.28$ J/g), 77 °C ($\Delta H = 1.90$ J/g) and 121 °C ($\Delta H = 12.32$ J/g) before melting for ***b*-DIPF**, ***o*-DIPF** and ***d*-DIPF**, respectively, indicating the 0D particles were presented in a metastable state (Fig. 4b, Fig. S7b and Fig. S9b). These results suggest the emission-quenched 0D particles may not be stable enough under

mechanical forces stimulation, and MRL turn-on behavior could be anticipated.

To evaluate the possible MRL characteristics of the 0D particles, their luminescence behaviors in the solid states were studied under mechanical stimuli. Upon grinding with a pestle, the ground sample of ***o*-DIPF** showed significantly enhanced emission accompanied with a blue-shifted of 22 nm. Notably, the Φ_F value of the ground sample reached 19.6 %, which was 163-fold higher than that of the pristine 0D particles, indicating a remarkable MRL turn-on behavior was realized (Fig. 4a). Similar results also observed in ***b*-DIPF** and ***d*-DIPF**. The ground samples of ***b*-DIPF** and ***d*-DIPF** showed intense emissions at 553 nm ($\Phi_F = 14.1\%$) and 539 nm ($\Phi_F = 6.91\%$), respectively (Fig. S7a, and Fig. S9a, Table 2). These results also suggest the length of alky chains in the molecules is important in terms of achieving high-contrast MRL behavior. Shorter or longer alky chain is inconvenient to quench the emission of their 0D particles and maximize the emission efficiency of their ground sample [52].

To identify the mechanism of the MRL turn-on of the 0D particles, the following experiments were carried out. Firstly, SEM image revealed the well-ordered 0D particles of ***o*-DIPF** were converted to random nanostructured aggregates under mechanical grinding (Fig. 5b). It was noted that such morphology and emission were quite similar to that of the emissive aggregates formed in THF/H₂O mixtures with 90% water. Secondly, powder X-ray diffraction (XRD) measurements revealed the different molecular arrangements of the pristine and the ground sample. As illustrated in Fig. 5c, the 0D particles displayed crystalline characteristic with poor crystallinity.

The peak around 25.1° with the d -spacing of about 3.53 \AA can be assigned to the π - π stacking of the aromatic rings. After being ground, the sharp peaks in the XRD pattern vanished. Correspondingly, a diffuse and broad diffraction were observed, suggesting the crystalline phase was transferred to an amorphous phase during mechanical grinding and the ordered molecules aggregates were converted into random motifs. In this process, the intermolecular π - π interactions in J -aggregates were disturbed, which resulted in the enhanced intensity as well blue-shifted of the fluorescence. In addition, the time-resolved emission-decay behaviors of the OD particles and ground sample were investigated and the fit results were summarized in Table 2. The shortened fluorescence lifetime of the solid in the ground form further demonstrated the well-ordered molecular packing was disturbed under mechanical grinding (Fig. 5d, Table 2). The radiative rate constants (K_r) of the ground solids were more than 10-times larger than those of the pristine OD particles, indicating the activation of radiative pathways in the molecular arrangements of the ground state.

3. Conclusion

In summary, a series of 1, 3-indandione-based A- π -D- π -A fluorene derivatives were designed and synthesized. Due to the balanced strength of the electron-donor and acceptor moieties, the compounds showed remarkable negative solvatochromic effect with red-shifted and intensified emission upon increasing the polarity of the solvents. The maximum fluorescence peak shifted above 130 nm accompanied with Φ_{FS} increasing over 35-times from nonpolar hexane to polar DMSO, making these compounds as prominent fluorescent probes for polarity detection. Interestingly,

aggregates with distinct fluorescence properties as well as nanostructured morphologies were obtained from THF/H₂O mixtures and by quickly removing their dichloromethane solvent under vacuum, respectively. The random nanostructures exhibited AIE characteristics, while the ordered 0D particles showed dramatically opposed emission quenching. Moreover, the non-emissive 0D particles exhibited remarkable MRL turn-on behavior, which was ascribed to the disturbance of the adverse π - π interactions and the activation of the emissive pathways. With the assistance of the alky effect, the ground sample of ***o*-DIPF** gave bright yellow emission at 556 nm with an Φ_F value of 19.6%, which was 163-fold higher than that of the pristine 0D particles. Our results indicate combining ICT effect of molecules with morphology control of the aggregates would be a promising strategy to obtain multifunctional fluorescent materials.

Acknowledgements

We thank the National Natural Scientific Foundation of China (NO.61605138), and the Shanxi Provincial Key Innovative Research Team in Science and Technology (NO.201513002-10).

References

- [1] Yagai S, Seki T, Aonuma H, Kawaguchi K, Karatsu T, Okura T, et al. Mechanochromic luminescence based on crystal-to-crystal transformation mediated by a transient amorphous state. *Chem Mater* 2016; 28: 234–41.
- [2] Wu H, Zhao P, Li X, Chen W, Ågren H, Zhang Q, et al. Tuning for visible fluorescence and near-infrared phosphorescence on a unimolecular mechanically

- sensitive platform via adjustable CH- π interaction. *ACS Appl Mater Interfaces* 2017; 9: 3865–72.
- [3] Sun H, Liu S, Lin W, Zhang KY, Lv W, Huang X, et al. Smart responsive phosphorescent materials for data recording and security protection. *Nat Commun* 2014; 5: 4601.
- [4] Jia J, Wu Y. Alkyl length dependent reversible mechanofluorochromism of phenothiazine derivatives functionalized with formyl group. *Dyes Pigments* 2017; 147: 537–43.
- [5] Xu J, Chi Z, editors. *Front Matter. RSC Smart Materials*, Royal Society of Chemistry, Cambridge; 2014.
- [6] Mao Z, Yang Z, Mu Y, Zhang Y, Wang Y-F, Chi Z, et al. Linearly tunable emission colors obtained from a fluorescent-phosphorescent dual-emission compound by mechanical stimuli. *Angew Chem, Int Ed* 2015; 54: 6270–3.
- [7] Chi Z, Zhang X, Xu B, Zhou X, Ma C, Zhang Y, et al. Recent advances in organic mechanofluorochromic materials. *Chem Soc Rev* 2012; 41: 3878.
- [8] Sagara Y, Yamane S, Mitani M, Weder C, Kato T. Mechanoresponsive luminescent molecular assemblies: an emerging class of materials. *Adv Mater* 2016; 28: 1073–95.
- [9] Tong S, Zhao S, He Q, Wang Q, Wang M-X, Zhu J. Fluorophores for excited-state intramolecular proton transfer by an yttrium triflate catalyzed reaction of isocyanides with thiocarboxylic acids. *Angew Chem, Int Ed* 2017; 56: 6599–603.

- [10] Li X, Tong X, Yin Y, Yan H, Lu C, Huang W, et al. Using highly emissive and environmentally sensitive o-carborane-functionalized metallophosphors to monitor mitochondrial polarity. *Chem Sci* 2017; 8: 5930–40.
- [11] Zhang Y, Li D, Li Y, Yu J. Solvatochromic AIE luminogens as supersensitive water detectors in organic solvents and highly efficient cyanide chemosensors in water. *Chem Sci* 2014; 5: 2710.
- [12] Karpenko IA, Niko Y, Yakubovskiy VP, Gerasov AO, Bonnet D, Kovtun YP, et al. Push–pull dioxaborine as fluorescent molecular rotor: far-red fluorogenic probe for ligand–receptor interactions. *J Mater Chem C* 2016; 4: 3002–9.
- [13] Wu H, Zhao P, Li X, Chen W, Ågren H, Zhang Q, et al. Tuning for visible fluorescence and near-infrared phosphorescence on a unimolecular mechanically sensitive platform via adjustable CH– π interaction. *ACS Appl Mater Interfaces* 2017; 9 :3865–72.
- [14] Jiang Y, Gindre D, Allain M, Liu P, Cabanetos C, Roncali J. A mechanofluorochromic push-pull small molecule with aggregation-controlled linear and nonlinear optical properties. *Adv Mater* 2015; 27: 4285–9.
- [15] Chen P-Z, Zhang H, Niu L-Y, Zhang Y, Chen Y-Z, Fu H-B, et al. A solid-state fluorescent material based on carbazole-containing difluoroboron β -diketonate: multiple chromisms, the self-assembly behavior, and optical waveguides. *Adv Funct Mater* 2017; 27: 1700332.
- [16] Jadhav T, Dhokale B, Patil Y, Mobin SM, Misra R. Multi-stimuli responsive donor–acceptor tetraphenylethylene substituted benzothiadiazoles. *J Phys Chem*

C 2016; 120: 24030–40.

- [17] Zhan Y, Gong P, Yang P, Jin Z, Bao Y, Li Y, et al. Aggregation-induced emission and reversible mechanochromic luminescence of carbazole-based triphenylacrylonitrile derivatives. *RSC Adv* 2016; 6: 32697–704.
- [18] Jayanty S, Radhakrishnan TP. Enhanced fluorescence of remote functionalized diaminodicyanoquinodimethanes in the solid state and fluorescence switching in a doped polymer by solvent vapors. *Chem Eur J* 2004; 10: 791–7.
- [19] Birks JB. *Photophysics of aromatic molecules*. London, U.K: Wiley; 1970.
- [20] Tracy HJ, Mullin JL, Klooster WT, Martin JA, Haug J, Wallace S, et al. Enhanced photoluminescence from group 14 metalloles in aggregated and solid solutions. *Inorg Chem* 2005; 44:2003–11.
- [21] Xue P, Sun J, Chen P, Gong P, Yao B, Zhang Z, et al. Strong solid emission and mechanofluorochromism of carbazole-based terephthalate derivatives adjusted by alkyl chains. *J Mater Chem C* 2015; 3: 4086–92.
- [22] Zhang Y, Li H, Zhang G, Xu X, Kong L, Tao X, et al. Aggregation-induced emission enhancement and mechanofluorochromic properties of α -cyanostilbene functionalized tetraphenyl imidazole derivatives. *J Mater Chem C* 2016; 4: 2971–8.
- [23] Yagai S, Okamura S, Nakano Y, Yamauchi M, Kishikawa K, Karatsu T, et al. Design amphiphilic dipolar π -systems for stimuli-responsive luminescent materials using metastable states. *Nat Commun* 2014; 5: 5013.
- [24] Srinivasan S, Babu PA, Mahesh S, Ajayaghosh A. Reversible self-assembly of

- entrapped fluorescent gelators in polymerized styrene gel matrix: erasable thermal imaging via recreation of supramolecular architectures. *J Am Chem Soc* 2009; 131: 15122–3.
- [25] Naito H, Morisaki Y, Chujo Y. o-carborane-based anthracene: a variety of emission behaviors. *Angew Chem, Int Ed* 2015;54:5084–7.
- [26] Kwon MS, Gierschner J, Yoon S-J, Park SY. Unique piezochromic fluorescence behavior of dicyanodistyrylbenzene based donor-acceptor-donor triad: mechanically controlled photo-induced electron transfer (ET) in molecular assemblies. *Adv Mater* 2012; 24: 5487–92.
- [27] Chung JW, You Y, Huh HS, An B-K, Yoon S-J, Kim SH, et al. Shear-and UV-induced fluorescence switching in stilbenic π -dimer crystals powered by reversible [2 + 2] cycloaddition. *J Am Chem Soc* 2009; 131: 8163–72.
- [28] Gawinecki R.; Viscardi, G.; Barni, E.; Hanna M A ,4- Tert-butyl-1-(4'-dimethylamino-benzylideneamino) pyridinium perchlorate (BDPP): a novel fluorescent dye. *Dyes Pigments* 1993; 23, 73-2.
- [29] Qi Q, Qian J, Tan X, Zhang J, Wang L, Xu B, et al. Remarkable turn-on and color-tuned piezochromic luminescence: mechanically switching intramolecular charge transfer in molecular crystals. *Adv Funct Mater* 2015; 25: 4005–10.
- [30] Hong Y, Lam JWY, Tang BZ. Aggregation-induced emission: phenomenon, mechanism and applications. *Chem Commun* 2009:4332.
- [31] Yang Y, Chen L, Jiang F, Wan X, Yu M, Cao Z, et al. Fabricating a super stable luminescent chemosensor with multi-stimuli-response to metal ions and small

- organic molecules through turn-on and turn-off effects. *J Mater Chem C* 2017; 5: 4511–9.
- [32] Tanioka M, Kamino S, Muranaka A, Ooyama Y, Ota H, Shirasaki Y, et al. Reversible near-infrared/blue mechanofluorochromism of aminobenzopyranoxanthene. *J Am Chem Soc* 2015; 137: 6436–9.
- [33] Qi Q, Liu Y, Fang X, Zhang Y, Chen P, Wang Y, et al. AIE (AIEE) and mechanofluorochromic performances of TPE-methoxylates: effects of single molecular conformations. *RSC Adv* 2013; 3: 7996.
- [34] Gundu S, Kim M, Mergu N, Son Y-A. AIE-active and reversible mechanochromic tetraphenylethene-tetradiphenylacrylonitrile hybrid luminogens with re-writable optical data storage application. *Dyes Pigments* 2017; 146: 7–13.
- [35] Wang J, Mei J, Hu R, Sun JZ, Qin A, Tang BZ. Click synthesis, aggregation-induced emission, E / Z isomerization, self-organization, and multiple chromisms of pure stereoisomers of a tetraphenylethene-cored luminogen. *J Am Chem Soc* 2012; 134: 9956–66.
- [36] Guo Y, Xu L, Liu H, Li Y, Che C-M, Li Y. Self-assembly of functional molecules into 1D crystalline nanostructures. *Adv Mater* 2015; 27: 985–1013.
- [37] Wang L, Wang K, Zou B, Ye K, Zhang H, Wang Y. Luminescent chromism of boron diketonate crystals: distinct responses to different stresses. *Adv Mater* 2015; 27: 2918–22.
- [38] Sagara Y, Kato T. Mechanically induced luminescence changes in molecular assemblies. *Nat Chem* 2009; 1: 605–10.

- [39] Li Y, Liu T, Liu H, Tian M-Z, Li Y. Self-assembly of intramolecular charge-transfer compounds into functional molecular systems. *Acc Chem Res* 2014; 47: 1186–98.
- [40] Wen P, Gao Z, Zhang R, Li A, Zhang F, Li J, et al. A- π -D- π -A carbazole derivatives with remarkable solvatochromism and mechanoresponsive luminescence turn-on. *J Mater Chem C* 2017; 5: 6136–43.
- [41] Cheng J, Zhang F, Li K, Li J, Lu X, Zheng J, et al. A planar dithiafulvene based sensitizer forming J-aggregates on TiO₂ photoanode to enhance the performance of dye-sensitized solar cells. *Dyes Pigments* 2017; 136: 97–103.
- [42] Cheng J, Cao Y, Liang X, Zheng J, Zhang F, Wei S, et al. Dithiafulvene-based organic sensitizers using pyridine as the acceptor for dye-sensitized solar cells. *Mater Chem Phys* 2017; 192: 349–55.
- [43] Guo K, Yan K, Lu X, Qiu Y, Liu Z, Sun J, et al. Dithiafulvenyl unit as a new donor for high-efficiency dye-sensitized solar cells: synthesis and demonstration of a family of metal-free organic sensitizers. *Org Lett* 2012; 14: 2214–7.
- [44] Guo K, Zhang F, Guo S, Li K, Lu X, Li J, et al. Achieving red/near-infrared mechanoresponsive luminescence turn-on: mechanically disturbed metastable nanostructures in organic solids. *Chem Commun* 2017; 53: 1309–12.
- [45] Xue P, Yao B, Sun J, Xu Q, Chen P, Zhang Z, et al. Phenothiazine-based benzoxazole derivatives exhibiting mechanochromic luminescence: the effect of a bromine atom. *J Mater Chem C* 2014; 2: 3942–50.
- [46] Tanaka M, Muraoka S, Matsui Y, Ohta E, Sakai A, Ogaki T, et al. Remarkable

- solvatochromism of a [2.2]paracyclophane-containing organoboron complex: a large Stokes shift promoted by excited state intramolecular charge transfer. *ChemPhotoChem* 2017; 1: 188–97.
- [47] Niko Y, Sasaki S, Narushima K, Sharma DK, Vacha M, Konishi G. 1-, 3-, 6-, and 8-tetrasubstituted asymmetric pyrene derivatives with electron donors and acceptors: high photostability and regioisomer-specific photophysical properties. *J Org Chem* 2015; 80: 10794–805.
- [48] Wang P, Wu S. A study on the spectroscopy and photophysics of 4'-N,N-dimethylaminoflavone derivatives. *J Lumin* 1994; 6233—39.
- [49] Guan XL, Jia TM, Zhang DH, Zhang Y, Ma HC, Lu DD, et al. A new solvatochromic linear π -conjugated dye based on phenylene-(poly)ethynylene as supersensitive low-level water detector in organic solvents. *Dyes Pigments* 2017; 136: 873–80.
- [50] Hu R, Lager E, Aguilar-Aguilar A, Liu J, Lam JWY, Sung HHY, et al. Twisted intramolecular charge transfer and aggregation-induced emission of BODIPY derivatives. *J Phys Chem C* 2009; 113: 15845–53.
- [51] Xu B, He J, Mu Y, Zhu Q, Wu S, Wang Y, et al. Very bright mechanoluminescence and remarkable mechanochromism using a tetraphenylethene derivative with aggregation-induced emission. *Chem Sci* 2015; 6: 3236–41.
- [52] An P, Shi Z-F, Dou W, Cao X P, Zhang H L. Synthesis of 1,4-Bis[2,2-bis(4-alkoxyphenyl) vinyl] benzenes and Side Chain Modulation of

Their Solid-State Emission. *Org Lett* 2010; 12: 4364–7.

ACCEPTED MANUSCRIPT

Tables

Captions

Table 1 Photophysical properties of the compounds in various solvents.

Table 2 Photophysical data of the solids in original and ground state.

Table 1

Comp.	Solvent	Δf	λ_{Abs} (nm)	ϵ ($10^4 \text{M}^{-1} \text{cm}^{-1}$)	FWHM (nm)	λ_{PL} (nm)	Stokes shift (cm^{-1})	Φ_{F} (%)
<i>b</i> -DIPF	Hexane	0	418	2.8	74	465	2278	0.9
	Toluene	0.012	437	6.3	81	492	2558	1.5
	Chloroform	0.149	445	6.1	88	527	3497	3.6
	THF	0.21	438	7.2	88	532	4034	4.9
	Acetone	0.28	435	6.8	90	564	5258	14.2
	DMSO	0.26	445	6.7	103	596	5693	29.7
<i>o</i> -DIPF	Hexane	0	419	5.4	74	462	2361	0.7
	Toluene	0.012	429	4.4	80	486	2734	1.1
	Chloroform	0.149	444	4.9	81	530	3655	1.4
	THF	0.21	436	5.0	83	531	4103	4.8
	Acetone	0.28	433	3.8	85	568	5489	11.6
	DMSO	0.26	441	3.7	97	596	5897	24.5
<i>d</i> -DIPF	Hexane	0	419	4.4	74	463	2268	0.8
	Toluene	0.012	429	4.6	81	490	2902	1.2
	Chloroform	0.149	438	5.0	86	529	3927	1.3
	THF	0.21	433	4.5	88	531	4262	4.6
	Acetone	0.28	429	3.4	90	566	5642	12.1
	DMSO	0.26	437	3.2	104	598	6161	22.8

Table 2

Comp.	Pristine 0D particles					Ground sample				
	λ_{PL} (nm)	Φ_{F} (%)	τ (ns)	K_{r} ($\times 10^{-5}$ ns^{-1})	K_{nr} (ns^{-1})	λ_{PL} (nm)	Φ_{F} (%)	τ (ns)	K_{r} ($\times 10^{-4}$ ns^{-1})	K_{nr} (ns^{-1})
<i>b</i> -DIPF	563	0.38	3.4	1.105	0.291	553	14.1	2.5	5.641	0.399
<i>o</i> -DIPF	578	0.12	2.9	4.124	0.344	556	19.6	1.8	1.034	0.531
<i>d</i> -DIPF	556	0.25	3.1	7.936	0.317	539	6.91	2.2	3.117	0.450

Captions

Scheme 1 Synthesis of compounds ***b*-DIPF**, ***o*-DIPF** and ***d*-DIPF**. i) DMSO, KOH, H₂O, TBAB, 1-bromobutane or 1-bromooctane or 1-bromododecane; ii) Pd(PPh₃)₄, K₂CO₃, H₂O, (CH₂OMe)₂, N₂, reflux; iii) 1,3-indanedione, piperidine, CH₃CH₂OH, reflux.

Fig. 1 (a) Geometrically optimized 3D molecular models and (b) HOMO (down) and LUMO (up) spatial distributions of ***o*-DIPF** by TD-DFT B3LYP/6-31G(d) calculation.

Fig.2 (a) UV-Vis absorption and (b) photoluminescence (PL) spectra of ***o*-DIPF** in various solvents (10 μM); (c) Luminescence photographs of ***o*-DIPF** in various solvents (10 μM) under UV irradiation at 365 nm; (d) Linear correlation of the orientation polarization (Δf) of solvent media with the Stokes shifts ($\Delta\nu$) for ***o*-DIPF**; (e) Commission Internationale de l'Eclairage (CIE) color coordinates of ***o*-DIPF** in various solvents on the chromatic diagram.

Fig.3 (a) Photograph of ***o*-DIPF** in THF/H₂O mixtures (10 μM) with different f_w taken under UV illumination ($\lambda_{ex} = 365$ nm); (b) Fluorescence spectra, (c) UV-Vis absorption spectra, and (d) PL intensity and λ_{PL} changes of ***o*-DIPF** in THF/H₂O mixtures (10 μM) different f_w ; (e) SEM images of ***o*-DIPF** in THF/ H₂O mixtures with $f_w = 90\%$.

Fig.4 (a) PL spectra of the pristine 0D particles and the ground sample of *o*-DIPF.

Insert: Fluorescence images of emission turn-on change of 0D particles of *o*-DIPF under mechanical force grinding; (b) DSC curve of pristine 0D particles of *o*-DIPF.

Fig.5 SEM images of (a) pristine 0D particles and (b) ground sample of *o*-DIPF; (c)

XRD patterns of pristine 0D particles and ground sample of *o*-DIPF; (d)

Time-resolved fluorescence spectra of pristine 0D particles and ground sample of *o*-DIPF.

Scheme 1

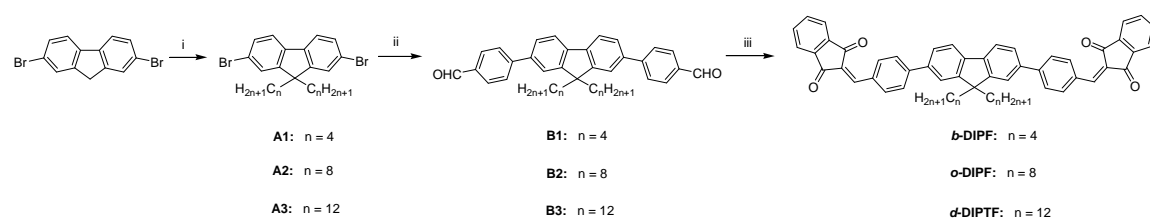


Figure 1

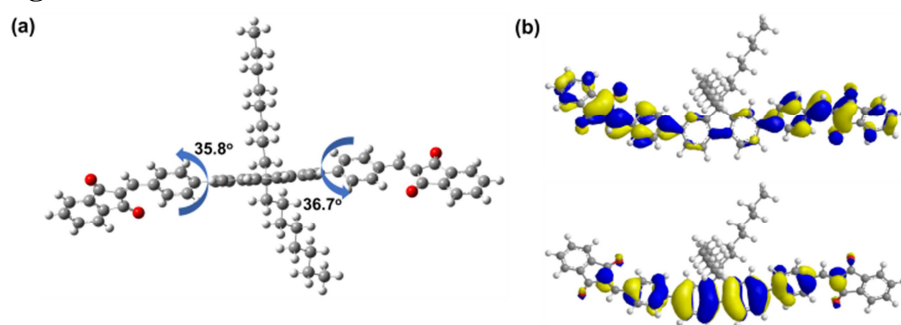


Figure 2

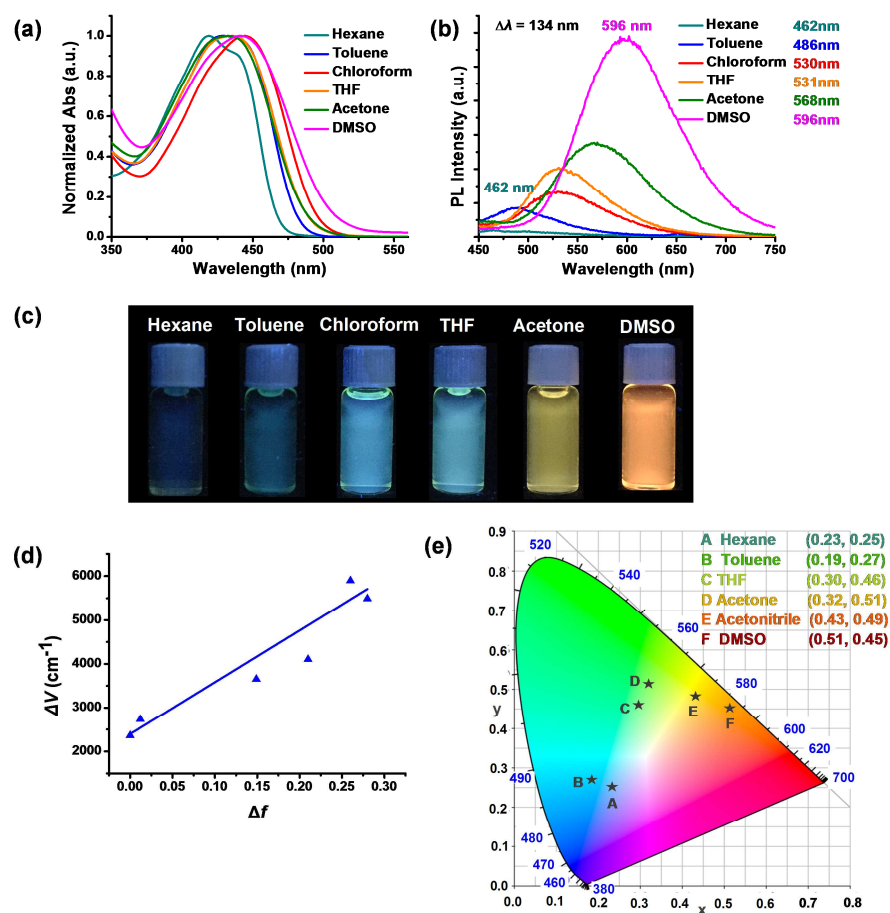


Figure 3

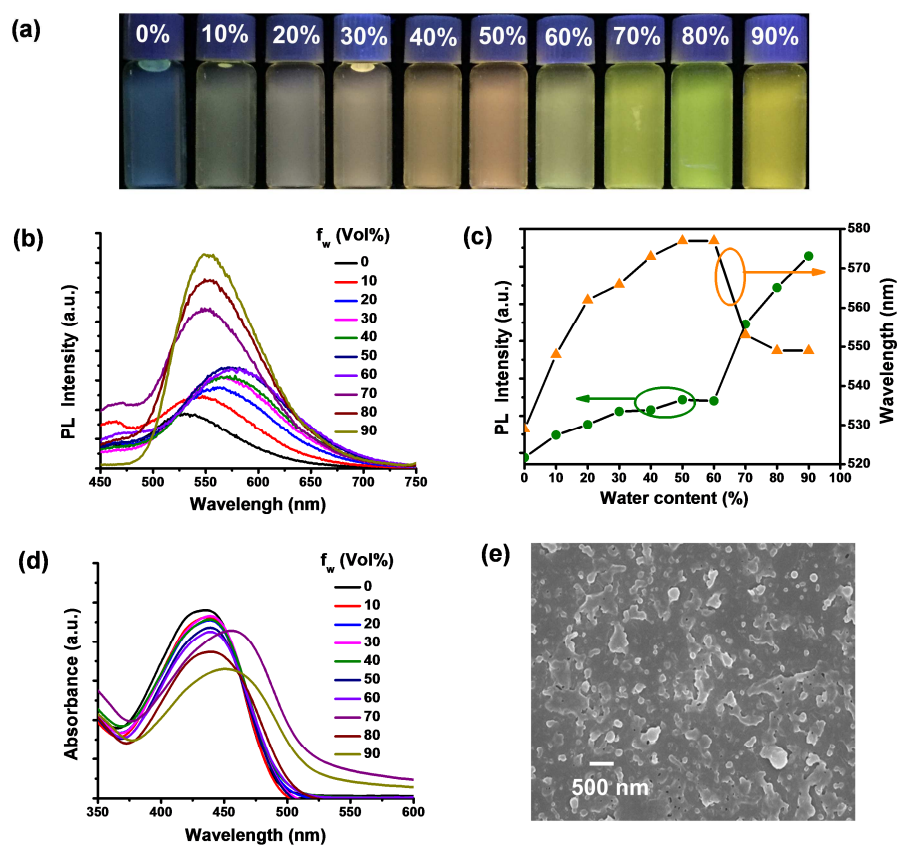


Figure 4

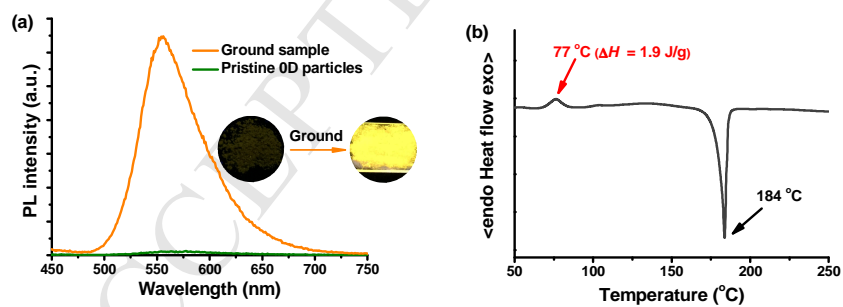
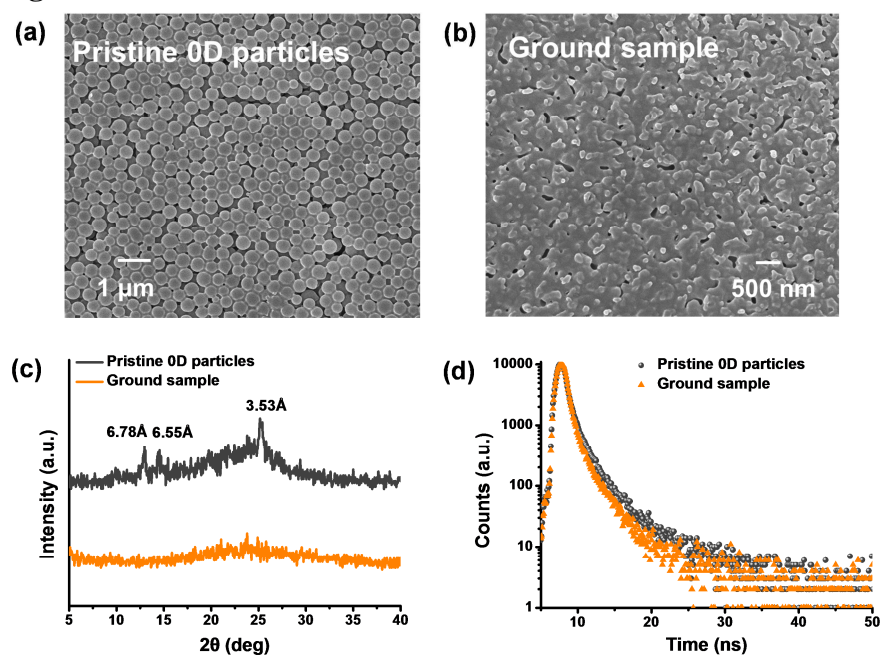


Figure 5



Highlights

- Organic luminophores exhibit versatile fluorescent behaviors in different states.
- The luminophores exhibit negative solvatochromism in solutions.
- The fluorescent behaviors in aggregates are determined by nanostructure morphologies.
- The random aggregates of the luminophores exhibit aggregation-induced emission.
- The 0D particles of the luminophores exhibit mechanoresponsive luminescence turn-on.